DOI: 10.1002/chem.200500592

Synthesis and Characterization of Dinuclear Ruthenium Complexes Covalently Linked to Ru^{II} Tris-bipyridine: An Approach to Mimics of the Donor Side of Photosystem II

Yunhua Xu,[a] Gerriet Eilers,[b] Magnus Borgström,[b] Jingxi Pan,[c] Maria Abrahamsson,[b] Ann Magnuson,[d] Reiner Lomoth,[b] Jonas Bergquist,[e] Tomáš Polívka,[c] Licheng Sun,[a] Villy Sundström,[c] Stenbjörn Styring,[d] Leif Hammarström,*[b] and Björn Åkermark*[a]

Abstract: To mimic the electron-donor side of photosystem II (PSII), three trinuclear ruthenium complexes (**2**, **2a**, **2b**) were synthesized. In these complexes, a mixed-valent dinuclear $Ru_2^{II,III}$ moiety with one phenoxy and two acetato bridges is covalently linked to a Ru^{II} tris-bipyridine photosensitizer. The properties and photoinduced electron/energy transfer of these complexes were studied. The results show that the $Ru_2^{II,III}$ moieties in the complexes readily undergo reversible one-electron reduction and one-electron oxidation to give the $Ru_2^{II,II}$ and $Ru_2^{III,III}$ states, respectively. This could allow for photooxidation of the sensitizer part with an external acceptor and subsequent electron transfer from the dinuclear ruthenium moiety to regenerate the sensitizer. However, all trinuclear ruthenium complexes have a very short excited-state lifetime, in the range of a few nanoseconds to less than 100 ps. Studies by femtosecond time-resolved techniques suggest that a mixture of intramolecular energy and electron transfer between the dinuclear ruthenium moiety and the excited $[Ru(bpy)_3]^{2+}$ photosensitizer is responsible for the short lifetimes. This problem is overcome by anchoring the complexes with ester- or carboxyl-substituted bipyridine ligands (**2a**, **2b**) to nanocrystalline TiO_2, and the desired electron transfer from the excited state of the $[Ru(bpy)_3]^{2+}$ moiety to the conduction band of TiO_2 followed by intramolecular electron transfer from the dinuclear $Ru_2^{II,III}$ moiety to photogenerated Ru^{III} was observed. The resulting long-lived $Ru_2^{III,III}$ state decays on the millisecond timescale.

Keywords: electrochemistry · electron transfer · mixed-valent compounds · ruthenium cluster · sensitizers

[a] Dr. Y. Xu, Prof. L. Sun,[+] Prof. B. Åkermark
Department of Organic Chemistry, Arrhenius Laboratories
Stockholm University, 106 91 Stockholm (Sweden)
Fax: (+46) 8-154-908
E-mail: bjorn.akermark@organ.su.se

[b] G. Eilers, M. Borgström, M. Abrahamsson, Dr. R. Lomoth, Prof. L. Hammarström
Department of Physical Chemistry, Uppsala University
Box 579, 751 23 Uppsala (Sweden)
E-mail: leifh@fki.uu.se

[c] Dr. J. Pan, Dr. T. Polívka, Prof. V. Sundström
Department of Chemical Physics, Lund University
Box 124, 221 00 Lund (Sweden)

[d] Dr. A. Magnuson, Prof. S. Styring
Molecular Biomimetics, Uppsala University
Villavägen 6, 752 36 Uppsala (Sweden)

[e] Prof. J. Bergquist
Institute of Chemistry, Department of Analytical Chemistry
Uppsala University, Box 599, 751 24 Uppsala (Sweden)

[+] Present address: Department of Chemistry
Royal Institute of Technology, 100 44 Stockholm (Sweden)

Introduction

One of the most important and fundamental chemical processes in nature is the oxidation of water to molecular oxygen in photosynthesis.[1–10] In plants and cyanobacteria, this reaction takes place in photosystem II (PSII). The electrons that PSII extracts from water are transferred to acceptors and used in the reduction of carbon dioxide to carbohydrates. In the primary photoreaction, light is absorbed by the chlorophyll pigment P_{680} in the core of PSII. This pigment acts as a single photoelectron donor and is regenerated after each photo-event by electron transfer from a tetranuclear manganese complex, where the actual oxidation of water takes place. The manganese complex binds water and transfers electrons one by one to the highly oxidizing P_{680}^{+}. After four electrons have been taken from the complex, molecular oxygen is released and the process is repeated. The

manganese complex in PSII is the only naturally occurring catalyst capable of water oxidation.

Only very few manganese-based molecular catalysts for water oxidation have so far been developed, and few have unequivocally been shown to oxidize water all the way to molecular oxygen without the aid of additional sacrificial agents.[5,7,11,12] Moreover, very few complexes of two or more manganese ions have been combined with a photosensitizer.[13–16] With the aim to create manganese-based, biomimetic molecular catalysts for water oxidation, we have prepared and investigated several supramolecular systems in which a mono- or dinuclear manganese complex is linked to a $[Ru(bpy)_3]^{2+}$-type photosensitizer.[13,14,17–25] Some related work has also been reported by Wieghardt et al.[15,16] In all of our linked ruthenium–manganese complexes, we have succeeded in observing light-induced, intramolecular electron transfer from the manganese moiety to the photogenerated $[Ru(bpy)_3]^{3+}$ center.[13,17,20,24] In addition, we were able to transfer three electrons, in a stepwise fashion, from the dinuclear manganese complexes to the ruthenium photosensitizer.[26] However, we have so far not been able to detect oxygen evolution with any of these complexes.

Manganese is abundant in the upper layers of the earth's crust, and is readily available to many living organisms in the biosphere. It may seem natural to copy nature's preference for manganese in photosynthetic water oxidation. However, it is interesting to note that so far the only synthetic materials shown to perform water oxidation to a reasonable extent by homogeneous chemical catalysis are dinuclear complexes of the second-row metal ruthenium.[6,7,11,27–30] In 1982, Meyer et al. reported a dinuclear ruthenium complex $[(bpy)_2(H_2O)RuORu(H_2O)(bpy)_2]^{4+}$ that can catalyze water oxidation, although the stability of the catalyst is limited to 10–25 turnovers.[27] Since then, a variety of related ruthenium complexes have been synthesized and shown to be water-oxidation catalysts.[6,7,11,28,29] Recently

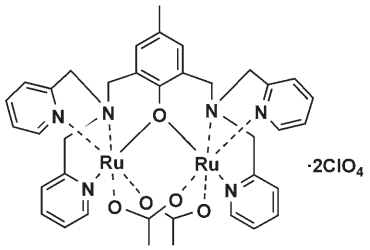

1

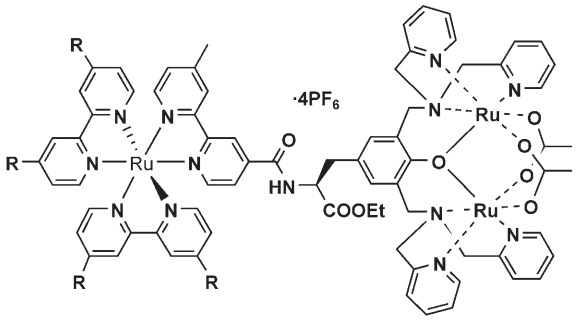

2 R=H
2a R=COOMe
2b R=COOH

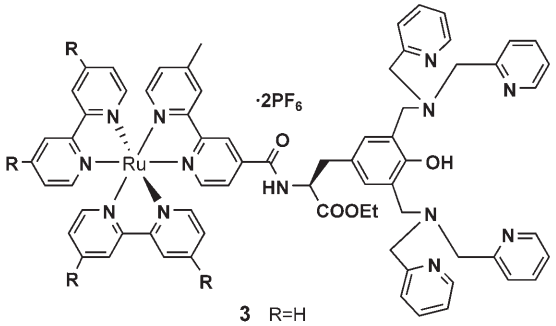

3 R=H
3a R=COOEt

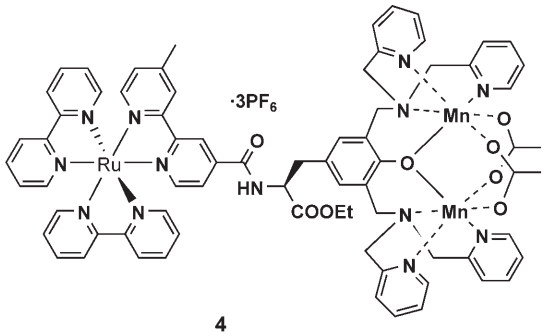

4

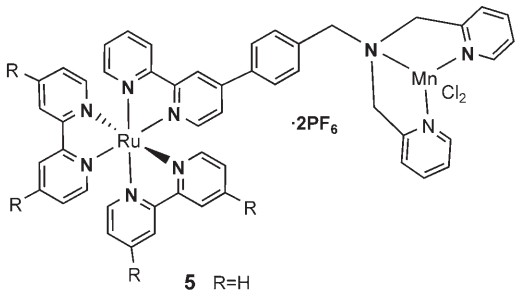

5 R=H
5a R=COOEt

Llobet et al. presented a new dinuclear ruthenium complex that is capable of oxidizing water to O_2 but does not contain the Ru-O-Ru motif.[30]

With the aim of improving the performance of the ruthenium complexes made by, for example, Meyer et al.,[27–29] and as an alternative route towards artificial photosynthesis, we previously prepared the dinuclear complex **1**,[31] and here we present a new trinuclear ruthenium complex **2**, which was synthesized by reaction of ligand complex **3**[21] with *cis*-$[RuCl_2(DMSO)_4]$. We also prepared the complexes **2a** and **2b**, which, in accordance with an earlier study on the dinuclear complexes **5** and **5a**,[24] would be expected to be less sensitive to excited-state quenching by the appended dinuclear complex. In addition, the carboxyl and ester groups allow for attachment to TiO_2 nanoparticles. The properties of these complexes and photoinduced electron transfer in the presence of TiO_2 as electron acceptor were studied, and the possibility of polyruthenium complexes as alternative electron donors in artificial systems is discussed.

Results and Discussion

Synthesis and characterization: Complex **1** was prepared as described earlier.[31] Ligand complexes **3** and **3a** were prepared by the published procedures.[21,32] By refluxing a mixture of **3** or **3a** with two equivalents of *cis*-$[RuCl_2(DMSO)_4]$ in MeOH in the presence of NaOAc, followed by addition of a saturated aqueous solution of NH_4PF_6, the trinuclear ruthenium complex **2** or **2a** was obtained. Complexes **2** and **2a** are ruthenium(II,II,III) complexes with one μ-oxo and two μ-acetato bridges, as shown by elemental analysis and ESI-MS. One of the Ru^{II} ions in the phenolic dimer was thus oxidized by air to Ru^{III} during preparation of the complex. Complex **2b** was obtained by hydrolysis of the ester groups of **2a**.

Redox properties of **2** in dry acetonitrile were studied by cyclic voltammetry (CV) and differential pulse voltammetry (DPV). The results are summarized in Table 1 and compared with the data for the previously published complex **1**. All potentials are given versus SCE. The observed ΔE_p values exceed somewhat the theoretical value of 59 mV for a reversible one-electron process, probably due to uncompensated solution resistance.

The CV of **2** shows six reversible redox waves (Figure 1). The irreversible wave at about −0.79 V is due to residual oxygen. The DPV of **2** shows six well-resolved peaks of equal shape and height, each equivalent to a one-electron transfer (not shown). Four waves are typical features of the $[Ru(bpy)_3]^{2+}$ moiety: one reversible oxidation wave ($E_{1/2}$ = 1.275 V) due to metal-centered oxidation ($Ru^{II} \rightarrow Ru^{III}$), and three reversible reduction waves ($E_{1/2}$ = −1.723, −1.489 and −1.196 V) from reduction of the bpy ligands. The remaining reversible oxidation wave ($E_{1/2}$ = 0.495 V) and reduction wave ($E_{1/2}$ = −0.191 V), which are similar to those of **1** (Figure 1),[31] are related to the dinuclear ruthenium moiety. In **1**, these waves were earlier shown to be due to oxidation ($Ru_2^{II,III} \rightarrow Ru_2^{III,III}$) and reduction ($Ru_2^{II,III} \rightarrow Ru_2^{II,II}$), respectively.[31] The shift to slightly more anodic potentials for **2**, as compared to **1**, is explained by the positive charge of the $[Ru(bpy)_3]^{2+}$ unit. Cyclic voltammetry was not performed on **2a** and **2b** due to lack of material, but data for other complexes $[Ru(bpy)_2(4\text{-Me-}4'\text{-X-bpy})]$ and the corresponding $[Ru(4,4'\text{-di-COOEt-bpy})_2(4\text{-methyl-}4'\text{-X-bpy})]$[13,24,33] show that the first reduction that is centered on the ester-substituted ligand lies at values 0.2 V less negative than the first ligand reduction in **2**, and that the $Ru^{3+/2+}$ potential is shifted by 0.3 V to more positive values. These values were used to estimate the driving force of the electron-transfer reactions discussed below.

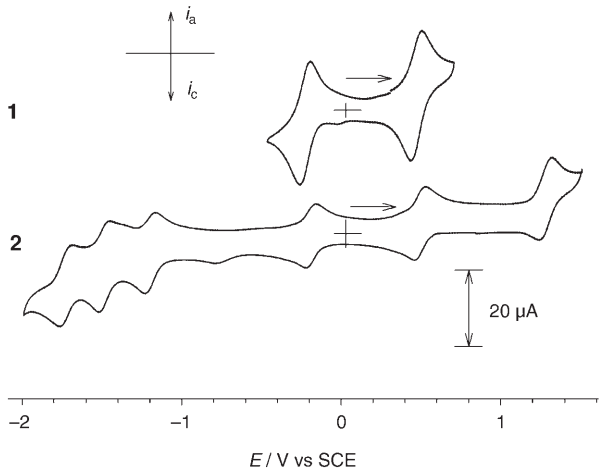

Figure 1. Cyclic voltammograms of **1** (1.7 mM) and **2** (1 mM) in CH_3CN containing 0.1 M nBu_4NPF_6. ν = 0.100 V s^{-1}.

The EPR data give further support for the assigned oxidation state of the dinuclear ruthenium moiety of complex **2**. The X-band EPR spectrum of **1** at low temperature (5 K), which was recently studied in detail,[31] displayed large rhombic g anisotropy with g_1 = 2.49, g_2 = 2.24 and g_3 = 1.85 (Figure 2) which is in agreement with a mixed-valent $Ru_2^{II,III}$ state. The EPR spectrum of **2** at low temperature (6 K) is very similar to that of **1**[31] and other mixed-valent $Ru_2^{II,III}$ ions,[34,35] and also showed large rhombic g anisotropy with g_1 = 2.49, g_2 = 2.25 and g_3 = 1.85 (Figure 2). These results thus indicate that the dinuclear ruthenium part of complex **2** is also a mixed-valent

Table 1. Electrochemical data for complexes **1** and **2**.

Complex	$E_{1/2}$ [V][a] (ΔE_p)[b]					
	$[Ru(bpy)_3]^{0/-}$	$[Ru(bpy)_3]^{+/0}$	$[Ru(bpy)_3]^{2+/+}$	$Ru_2^{II,III/II,II}$	$Ru_2^{III,III/II,III}$	$[Ru(bpy)_3]^{3+/2+}$
1[c]	–	–	–	−0.230 (70)	0.470 (70)	–
2[d]	−1.723 (74)	−1.489 (72)	−1.196 (62)	−0.191 (62)	0.495 (69)	1.275 (72)

[a] Versus SCE in CH_3CN solution with 0.1 M $[NnBu_4]PF_6$ as supporting electrolyte, ±0.02 V. [b] ν = 100 mV s^{-1}. [c] As ClO_4^- salt. [d] As PF_6^- salt.

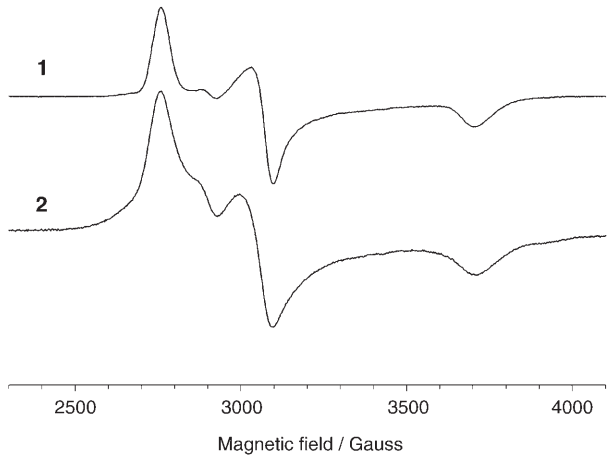

Figure 2. EPR spectra of **1** and **2** (1 mM) in CH_3CN. Temperature: 6 K; microwave frequency: 9.48 GHz; microwave power: 0.2 mW; modulation amplitude: 10 G.

$Ru_2^{II,III}$ core in the expected $S=1/2$ ground state, as suggested by the analytical data and also discussed previously for **1**.[31]

The UV/Vis absorption spectra of **1** and **2** in dry acetonitrile are shown in Figure 3. In both cases the dinuclear unit

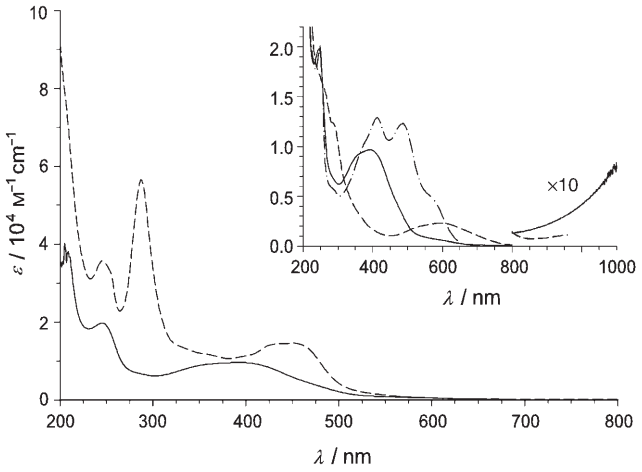

Figure 3. Absorption spectra of **1** (solid line) and **2** (dashed line) in CH_3CN. Inset: Absorption spectra of **1** in different redox states: $Ru_2^{II,III}$ (solid), $Ru_2^{III,III}$ (dashed) and $Ru_2^{II,II}$ (dot-dashed). Measured in a 1 mm cell in CH_3CN with 0.1 M $TBAPF_6$.

is in the mixed-valent $Ru_2^{II,III}$ oxidation state. Spectra of the dinuclear complex **1** in different oxidation states were reported earlier[31] and are shown as an inset. The $Ru_2^{II,II}$ state shows two absorption maxima at 410 and 490 nm, which were assigned to MLCT transitions.[31] The isovalent $Ru_2^{III,III}$ has a broad weak absorption at 600 nm ($\varepsilon=2300\,M^{-1}\,cm^{-1}$), which was assigned to a LMCT transition. The strongly coupled mixed-valent $Ru_2^{II,III}$ state is characterized by an absorption band at 380 nm, and the blue edge of an intervalence band is seen in the near-infrared region. In the spectrum of **2** the absorption of the dinuclear moiety is superimposed on the well-known MLCT (ca. 460 nm) and ligand-based transitions (290 nm) of the $[Ru(bpy)_3]^{2+}$ sensitizer.[36,37] The spectrum of **2** agrees well with the sum of the spectra for **1** and the $[Ru(bpy)_3]^{2+}$ moieties.

Emission spectroscopy: Complex **2** was excited at 460 nm, at the MLCT band of the $[Ru(bpy)_3]^{2+}$ chromophore. This unit displayed a weak emission in deoxygenated acetonitrile, with a maximum at about 670 nm. However, the intensity was strongly quenched and reached only about 0.5% of that of an isoabsorptive solution of $[Ru(bpy)_3](PF_6)_2$. The emission intensity of the precursor complex **3**, in which the dinuclear Ru complex has not yet been coordinated, was very similar to that of $[Ru(bpy)_3](PF_6)_2$. This shows that the coordinated Ru_2 unit strongly quenches the MLCT excited state of the $[Ru(bpy)_3]^{2+}$ chromophore. The result for **2a** was very similar to that for **2**, but with a red shift of the emission by about 10 nm due to the electron-withdrawing ester substituents.

Time-resolved spectroscopy: The emission decay kinetics for **2, 2a** and **2b** were investigated by time-correlated single-photon counting. By exhaustive electrolysis directly in the optical cell, the oxidation state of the dinuclear ruthenium unit was set to either $Ru_2^{II,II}$, $Ru_2^{II,III}$ or $Ru_2^{III,III}$. The emission decay traces were fitted to a sum of exponentials. The two shorter components dominated, and their lifetimes and relative amplitudes are given in Table 2. These lifetimes are on

Table 2. Emission lifetimes in the different redox states of the Ru_2 unit.

Complex	Emission lifetimes/ns (rel. amplitude)[a]		
	$Ru_2^{II,II}$ state	$Ru_2^{II,III}$ state	$Ru_2^{III,III}$ state
2	0.06 (60%)	0.15 (74%)	<0.05 ps (58%)
	0.63 (24%)	1.2 (15%)	0.35 (23%)
			3.0 (10%)
2a	0.45 (75%)	0.4 (75%)	1.2 (72%)
	3.0 (24%)	3 (27%)	5 (24%)
2b	–[b]	<0.05 (43%)	–[b]
		0.5 (22%)[c]	

[a] In acetonitrile. Minor components ($\leq$10%) with lifetimes of >10 ns are not given; see text. [b] Not measured. [c] Long-lived components with more than 10% of the amplitude were present.

the timescale of a few nanoseconds to less than 100 ps, which is much shorter than that of about 1200 ns observed for **3**[21] and shows the strong quenching of the $[Ru(bpy)_3]^{2+}$ emission by the dinuclear Ru complex. The reason for the multi-exponential emission decay, with the presence of minor components on the timescale of 1–10 ns and above, may be either the conformational flexibility of the link between the $[Ru(bpy)_3]^{2+}$ and Ru_2 units, which results in a range of relative distances and orientations, or partial rearrangements of the dinuclear complex moiety that lead, for example, to partial loss of acetate and/or change of coordination mode in solution. The latter explanation is supported by the fact that addition of small amounts (<1%) of water strongly affected the emission decay curves, increasing the

long-lived components. Importantly, a complex very similar to **2**, but with two of the pyridine ligands of the Ru_2 moiety exchanged for phenolate, displayed a very similar multi-exponential emission decay in the initial redox state $Ru_2^{III,III}$.[38] When reduced to the $Ru_2^{II,III}$ state, however, the emission decay became perfectly single exponential (99.8% of the amplitude) with a lifetime of 4 ns. Notably, there was a delay of a few minutes between complete electrochemical reduction and the simplification of the decay to a single exponential. This suggests that the Ru_2 complex did undergo coordination changes on a timescale of a few minutes when reduced to the $Ru_2^{II,III}$ state, for instance, change in acetate coordination, as discussed above, to give a single complex structure also in solution. This shows that the multi-exponential decay is not simply due to impurities or experimental artefacts, but is an intrinsic property of the complex in solution.

The complexes were also investigated by femtosecond transient absorption spectroscopy in their initial $Ru_2^{II,III}$ state. The transient spectra of **2** and **2a** after excitation at 490 nm are shown in Figure 4. At 10 ps after excitation the spectra show bleaching of the MLCT band of the $[Ru(bpy)_3]^{2+}$ unit around 450 nm (470 nm for **2a**) and a positive transient absorption above 500 nm (above 520 nm for **2a**). These transient signals were significantly smaller after 400 ps, and for **2** the fact that the shape of the spectrum remained the same as after 10 ps indicated decay to the ground state. For **2a**, however, the shape of the signal at 400 ps was somewhat different, and at 530 nm the signal was even higher than after 10 ps. The transient trace at this wavelength (Figure 5b) showed a clear rise-and-decay behavior, which could be fitted to simple two-step consecutive kinetics (A→B→C) with time constants for rise and decay of $\tau = 350$ ps and $\tau = 1580$ ps, respectively. For **2b**, the rise and decay around 530 nm were much smaller in amplitude (Figure 5c), but gave similar time constants of $\tau = 250$ ps and $\tau = 1490$ ps, respectively. Finally, for **2**, no rise at all was observed around this wavelength, and the bleaching recovery could be fitted to biexponential kinetics with $\tau_1 = 55$ ps and $\tau_2 = 290$ ps and equal amplitudes for the components (Figure 5a).

The bleaching recovery kinetics of the three complexes are in fair agreement with those observed in the emission decays. With a multi-exponential decay behavior, and component lifetimes that are on the order of the response function of the emission experiments, perfect agreement cannot be expected. Thus, the dominant 150 ps component in the

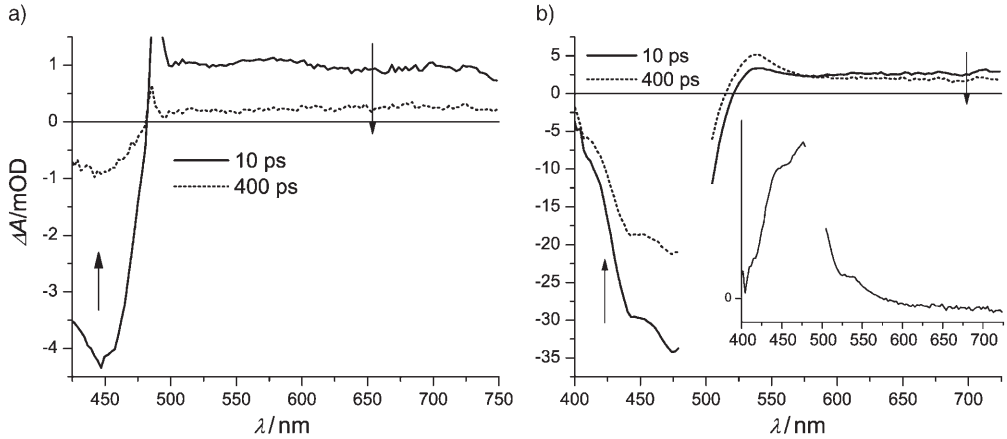

Figure 4. a) Transient absorption spectra of **2** recorded at 10 ps (solid line) and 400 ps (dashed line) after excitation at 490 nm. b) The corresponding spectra of **2a**. The inset shows the difference obtained by subtracting the two spectra at 10 ps and 400 ps. Arrows shows the direction of the time evolution of the signal.

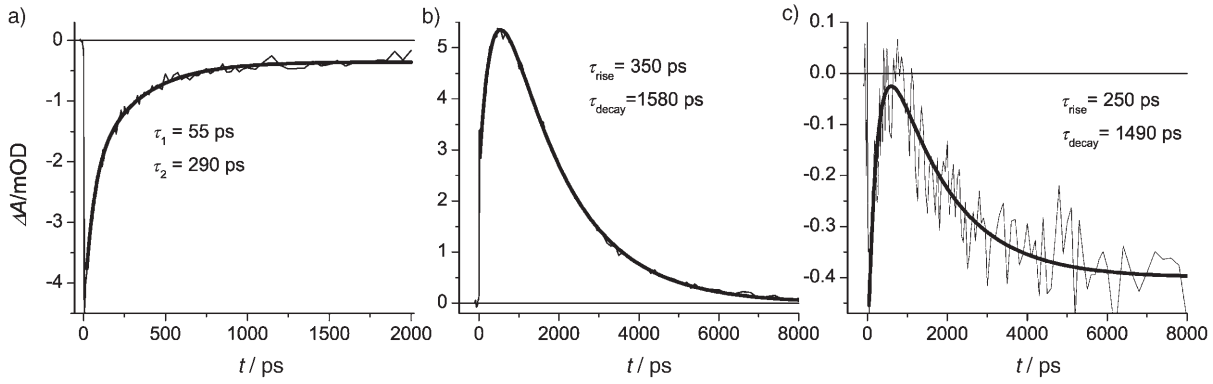

Figure 5. a) Kinetics indicating no product formation for **2**; decay of the excited state is shown as bleaching recovery at 450 nm. b) and c) Kinetics showing formation and decay of the electron-transfer product for **2a** and **2b**, respectively. Kinetics in panels b) and c) were recorded at 530 nm. Thick lines correspond to fits.

emission decay of **2** probably represents a weighted average of the 55 and 290 ps components of bleaching recovery (attributed to excited-state decay), while the small 1.2 ns emission component is poorly resolved in the transient absorption experiment. At the end of the optical delay, after 8 ns, about 10% of the ground state bleaching remained, consistent with the presence of about 10% of emission components with lifetimes above a few nanoseconds. For **2a** the agreement is also good, but the minor, approximately 3 ns, component in the emission decay is probably masked by the approximately 1.6 ns transient absorption component attributed to decay of the intermediate (see above). For **2b** both methods indicate a relatively large fraction (ca. one-third) of complexes with a much longer lifetime (>10 ns). Presumably, the preparation of **2b** by hydrolysis of **2a** resulted in partial demetallation of the Ru_2 site, or even breaking of the amide bond that attaches this complex to the $[Ru(bpy)_3]^{2+}$ unit. This would then decrease or even eliminate emission quenching and lead to a longer lifetime in a fraction of the complexes.

The inset of Figure 4b shows the difference in transient absorption at 400 ps and 10 ps for complex **2a**. This double-difference spectrum displays mainly the features of the $[Ru(bpy)_3]^{2+}$ ground state, showing that most of the excited state decay regenerates the ground state on this timescale. In addition, there is a relatively weak absorption around 530 nm that tails off towards the red. This is not the product of energy-transfer quenching by the Ru_2 unit (i.e., a $[Ru_2(bpmp)Ac_2]^{+}$ excited state), because direct excitation of **1** revealed only very short lived ($\tau \approx 6$ ps) transients (not shown).[39] Instead it must be attributed to electron-transfer products (see below).

Quenching mechanisms: As indicated in the introduction, the aim with complex **2** was to mimic fundamental PSII reactions by photooxidizing the $[Ru(bpy)_3]^{2+}$ unit—initially with an external electron acceptor—and to use this to drive intramolecular oxidation of a potentially catalytic Ru_2 complex. However, a crucial property is the excited-state lifetime of the complexes, which is intimately linked to the possibility of generating intermediate $[Ru(bpy)_3]^{3+}$ complexes by oxidative quenching by an external electron acceptor. Since we have earlier shown that the excited state of the $[Ru(bpy)_3]^{2+}$ chromophore is quenched by appended monomeric and dimeric manganese complexes,[8,13,24] we anticipated a similar result also for **2**. The quenching rate was, however, much faster in all investigated oxidation states of **2** than for the previously investigated $RuMn_2^{II,II}$ complex **4**[13]. The latter displayed an excited-state lifetime of 110 ns for the dominant component, which is three orders of magnitude longer than the main lifetime of **2** ($\tau \approx 150$ ps), in spite of the fact that both complexes are based on the same structure. The dinuclear ruthenium moiety of complex **2** is thus a much more efficient quencher than the corresponding dinuclear manganese complex, and it is important to elucidate the mechanisms responsible for this difference.

Two types of quenching mechanisms must be considered: electron-transfer (ET) and energy-transfer (EnT) quenching. Heavy-atom quenching can be excluded, because Ru is already present in the $[Ru(bpy)_3]^{2+}$ chromophore itself, and paramagnetic quenching is not likely, as the diamagnetic $Ru_2^{II,II}$ state is an equally efficient quencher as the $Ru_2^{II,III}$ state. The Coulombic (Förster) mechanism of energy transfer can be excluded, as the direct calculation of the rate from the transition dipole moments and the spectral overlap of the $[Ru(bpy)_3]^{2+}$ emission and the Ru_2 absorption[40] for all oxidation states of **2**, **2a**, and **2b** gives predicted rates on the timescale of 100 ns, much slower than the observed ones. In contrast the rate constant for the exchange (Dexter) mechanism cannot be directly calculated from the spectra and may be operative in this case. Note that the excited state of the Ru_2 complex **1** was very short lived ($\tau =$ 6 ps) and nonemissive, so that no observable EnT products are expected. Quenching by ET is also possible, and the driving force for the possible reactions was calculated with the standard Weller equation: $-\Delta G^0 = E_{00} - e(E_D^0 - E_A^0)$, where E_{00} [eV] is the excited-state energy of the $[Ru(bpy)_3]^{2+}$ unit, estimated from the maximum of the emission spectrum at 77 K of the corresponding unquenched reference complexes **3** ($E_{00} = 2.1$ eV) and **3a** ($E_{00} = 2.0$ eV), and E_D^0 and E_A^0 are the formal potentials for the electron donor and acceptor, respectively, determined by cyclic voltammetry (see above and Table 1). Thus, in the $Ru_2^{II,III}$ state there is a significant driving force for both oxidative ($-\Delta G^0 =$ 0.65 eV for **2**) and reductive ($-\Delta G^0 = 0.40$ eV for **2**) ET quenching. In the $Ru_2^{II,II}$ state, only reductive quenching is possible ($-\Delta G^0 = 1.10$ eV for **2**), while the opposite is true for the $Ru_2^{III,III}$ state ($-\Delta G^0 = 1.35$ eV). For **2a** oxidative quenching is about 0.3 eV less favorable than in **2**, while reductive quenching has a driving force that is about 0.2 eV larger. The values for **2b** should be intermediate, but closer to those for **2a**.

We used the transient absorption data and the variation of excited-state lifetime between **2**, **2a** and **2b** to determine which quenching mechanism(s) is(are) operative in the different redox states. In the $Ru_2^{II,III}$ state the intermediate observed in transient absorption around 530 nm must be due to ET. If this is an oxidative quenching most of the intermediate absorption above 500 nm would be due to reduction of the Ru_2 unit, for which the $Ru_2^{II,II} - Ru_2^{II,III}$ absorption difference would give a band around 500 nm ($\Delta\varepsilon \approx 5 \times 10^3\,M^{-1}\,cm^{-1}$, see inset of Figure 3). For reductive quenching, most of the transient absorption would be due to the formation of the reduced $[Ru(bpy)_3]^{+}$ complex with a band around 510 nm ($\Delta\varepsilon \approx 1 \times 10^4\,M^{-1}\,cm^{-1}$).[36,37] The main result of the quenching, however, is the regeneration of the ground state $[Ru(bpy)_3]^{2+}$, also in the case of **2a** (Figure 4b, inset). This shows that at least one additional quenching mechanism operates in parallel but does not lead to long-lived, observable products. From a comparison of the initial excited-state bleaching at 450 nm (for **2**) or 470 nm (for **2a** and **2b**) after 10 ps ($\Delta\varepsilon \approx 1 \times 10^4\,M^{-1}\,cm^{-1}$)[41] and the maximum amplitude of the reduced $[Ru(bpy)_3]^{+}$ intermediate at

530 nm, it seems that reductive quenching may account only for about 15–25% of the total quenching reaction in **2a**, as little as 2–3% in **2b**, while for **2** no intermediates at all could be observed. In contrast to this substantial difference in ET yield, the excited-state lifetime varied only little; **2** has the lowest and **2a** the highest value. This suggests that the rate of the dominant quenching reaction, which did not lead to observable products but has the larger influence on the net quenching rate, increases slightly in the order **2a**< **2b**<**2**, while the observed ET reaction shows a larger variation in rate and in the opposite order: **2**<**2b**<**2a**. As the ET products give only small changes in transient absorption compared to $[Ru(bpy)_3]^{2+}$ recovery (Figure 4b, inset) we cannot determine whether it is oxidative or reductive quenching from the spectra. However, we suggest below that it is probably a reductive quenching leading to $[Ru(bpy)_3]^{+}$ and $Ru_2^{III,III}$ intermediates, while the dominant quenching mechanism is either exchange EnT or ET to the Ru_2 unit.

In the lowest excited state of $[Ru^{II}(bpy)_3]$ complexes, which is a triplet metal-to-ligand charge transfer (^{3}MLCT) state, the excess electron is localized on the ligand that is easiest to reduce.[36,37] Hopping between isoenergetic ligands is rapid, on the timescale of tens of picoseconds[42,43] or probably even much faster, as was recently discussed.[44] Thus, through-bond ET or EnT (Dexter) from the excited state complex to an acceptor linked to one of the bipyridine ligands will occur by first localizing the MLCT state on that ligand from which ET or EnT then occurs. As hopping is rapid, the observed rate is generally given by the equilibrium fraction of MLCT states localized on that ligand (a Boltzmann population) multiplied by the intrinsic rate constant for ET or EnT from that ligand[45] (cf. also the results of Kelly and Rogers[46]). For exchange EnT or oxidative ET, an electron should be transferred from the bipyridine to the Ru_2 unit. In **2**, the MLCT state will already be predominantly localized on the substituted, bridging bipyridine due to the electron-withdrawing amide group, as shown earlier by spectroscopic and electrochemical data for the same type of chromophore.[13,24] In **2a** and **2b**, the two electron withdrawing groups on each of the nonbridging bipyridines will instead localize the MLCT state preferentially on these ligands.[24] This will reduce the observed quenching rate, and we have used this effect with success in the RuMn complex **5a**[24] to reduce the quenching rate by almost three orders of magnitude as compared to **5**. For a reductive quenching, the effect of the substituents would be the opposite, as an electron should be transferred from the Ru_2 unit to a metal-based orbital of the excited $[Ru(bpy)_3]^{2+}$. This reaction would most likely be slower if the MLCT state is localized in the bridging ligand, so that the ligand mediating through-bond ET is already formally reduced. Based on this argument one would expect **2a** to give the fastest reaction and **2** the slowest. This is exactly what is observed for ET quenching giving detectable intermediates, and we therefore assign that process to reductive quenching. The dominant quenching instead follows the trend expected for exchange EnT and oxidative ET. If the recombination reaction after oxidative ET is very rapid ($\tau<100$ ps), as in the $Ru_2^{II,III}$ excited state decay, neither of them would give detectable products, and we cannot discriminate between these two mechanisms.

For the $Ru_2^{II,II}$ and $Ru_2^{III,III}$ state of the complexes no transient absorption data are available. In the former state, oxidative quenching can be excluded, however, as the $Ru_2^{II,II}$ complex cannot be further reduced by excited $[Ru(bpy)_3]^{2+}$. In addition, the fact that the excited state lifetimes are about ten times longer in **2a** than in **2** is inconsistent with the expected trend for reductive quenching, as described above. Thus, we assign the quenching in the $Ru_2^{II,II}$ state to (predominantly) exchange EnT. Similarly, for the $Ru_2^{III,III}$ state reductive quenching is not possible. The fact that the excited-state lifetimes are about one order of magnitude longer in **2a** than in **2** is consistent with both EnT and oxidative ET, and we cannot discriminate between these two mechanisms.

To conclude, the quenching of the $[Ru(bpy)_3]^{2+}$ excited state in the investigated complexes occurs by different mechanisms (EnT and oxidative or reductive ET) depending on the oxidation state of the Ru_2 moiety. In the $Ru_2^{II,III}$ state our data suggest that at least two different mechanisms are operative in parallel. Only the minor, reductive quenching gave rise to detectable products, that is, $[Ru(bpy)_3]^{+}$ and $Ru_2^{III,III}$, which recombined with a lifetime of 1–2 ns. Previously, we reported that exchange EnT quenching of the $[Ru(bpy)_3]^{2+}$ excited state by the mononuclear manganese in complex **5** was decreased by a factor of about 600 when the nonbridging bipyridines were substituted with ester groups (**5a**).[24] It is surprising that the improvement in excited-state lifetime obtained with the same strategy in the present study is much smaller: the lifetime of **2a** is only about ten times longer than that of **2**. This may be explained, however, by the fact that the bridging bipyridine ligand in the present complexes **2** is about 100 mV easier to reduce than that in **5**. This will increase the Boltzmann population of the bridge-localized MLCT state in **2a** by a factor of about 50 as compared to **5a**, and thus explains the around 50 times smaller enhancement of the excited-state lifetime. An obvious conclusion of these results is that the bridging bipyridine should be designed without electron-withdrawing groups, so that the MLCT state is more strongly localized on the nonbridging bipyridines. In this way quenching by both exchange EnT and oxidative ET will be reduced, and the excited state lifetime may be long enough for the desired photooxidation of $[Ru(bpy)_3]^{2+}$ by an external acceptor, as we have done in our previous studies.[8] In the present case, however, we need to use an electron acceptor that is faster than what can be obtained in a bimolecular, diffusional reaction, so that it may be efficient on the short timescale of the excited-state lifetime. Although some photooxidation of the $[Ru(bpy)_3]^{2+}$ unit may be possible to observe with a high concentration of, for example, methylviologen as acceptor, this method would selectively sample the minor, longer lived excited state components which may not be representative of the sample.

Photoinduced ET on nanocrystalline TiO_2: The carboxyl and ester groups at the $[Ru(bpy)_3]^{2+}$ moiety of complexes **2a** and **2b** offer the possibility of attachment to nanostructured TiO_2, which is known to accept electrons from ruthenium dyes with injection times on the order of femtoseconds to picoseconds.[47–50] Transient absorption spectra of **2a** attached to a TiO_2 film (**2a**-TiO_2) system are shown in Figure 6. Although no spectral features corresponding to formation of $Ru_2^{III,III}$ could be observed on the picosecond timescale after excitation, a new transient absorption band is observed at 300 ns delay. The spectral profile of this band matches that of the $Ru_2^{III,III}$ state[31] (Figure 3, inset), that is, the dinuclear ruthenium moiety is oxidized after excitation. In accordance with recent studies on TiO_2 sensitized by molecular dyads,[32,51–54] we propose the following scheme for $Ru_2^{III,III}$ formation: First, excitation of the $[Ru(bpy)_3]^{2+}$sensitizer is followed by electron injection into the conduction band of TiO_2 to give the $Ru_2^{II,III}$-$[Ru^{III}(bpy)_3]$-$TiO_2(e^-)$ state. This is consistent with the transient absorption spectrum after 200 ps, which shows ground-state bleaching below 530 nm and weak absorption above 530 nm due to $[Ru^{III}(bpy)_3]$ and the electrons in the TiO_2 conduction band. Then a second electron transfer from the $Ru_2^{II,III}$ moiety gives the final charge-separated state $Ru_2^{III,III}$-$[Ru^{II}(bpy)_3]$-$TiO_2(e^-)$, which is characterized by a long lifetime of $\tau_{1/2} \approx 1$ ms (Figure 6) and for which the expected $Ru_2^{III,III} - Ru_2^{II,III}$ absorption difference (Figure 3) matches well the transient spectrum observed after 300 ns (Figure 6). Although we can not precisely determine the rate constant for the second electron transfer, we can conclude that the rate lies in the range $10^9 > k > 10^7\ s^{-1}$, since its kinetic component is too fast to be resolved by nanosecond flash photolysis (resolution limit ca. 50 ns) and too slow for detection in the femtosecond experiment (upper limit ca. 700 ps in this particular experiment). The final step is charge recombination, which in Ru/TiO_2 systems is highly nonexponential and depends on many parameters.[55] Nevertheless, as is shown in the inset of Figure 6, for the **2a**-TiO_2 system the resulting charge-separated state has a very long lifetime and decays on the millisecond timescale. Similar results have been obtained also for the **2b**-TiO_2 system (data not shown). Under the conditions of the experiment in Figure 6 charge recombination with similar Ru complexes, but without an appended electron donor, occurs in less than 100 μs.[32] The much slower recombination in **2a** and **2b** is a significant improvement, and is comparable to the recombination rates of highly efficient TiO_2 sensitizers such as RuN3.[47,55] It is also comparable to the slow recombination rates observed for previous systems with Ru–donor dyads as TiO_2 sensitizers.[32,51–54] Note, however, that the ground-state recovery kinetics measured for **2a** and **2b** in the femto- to picosecond time domain do not show significant differences when going from solution to TiO_2 (data not shown), and this suggests that the primary electron injection is rather inefficient. Due to the multi-exponential character of these kinetics and poorer signal/noise ratio for the **2a**(**2b**)-TiO_2 system it was impossible to precisely determine the injection efficiency, but it clearly does not exceed 10%. Nevertheless, this system is a promising starting point for the development of entirely Ru-based systems for mimicking the donor side reactions of PSII.

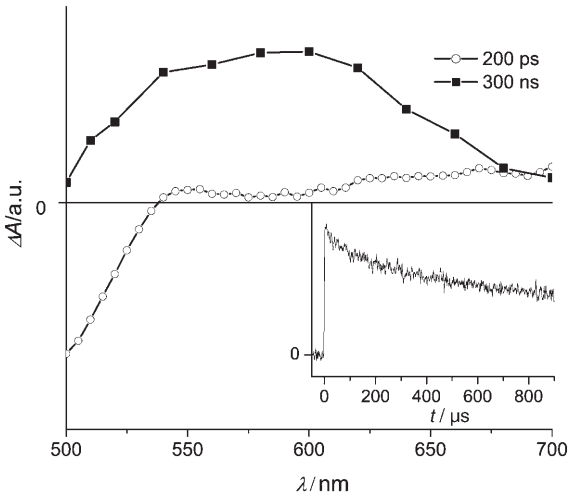

Figure 6. Transient absorption spectra of **2a**-TiO_2. Femtosecond excitation at 490 nm was used to obtain the transient spectrum at 200 ps, while 7 ns excitation pulses centered at 480 nm were used for measurements on the nanosecond timescale. The inset shows decay of the product monitored at 600 nm.

Conclusion

Efficient electron transfer from the sensitizer to the acceptor is crucial for the development of PSII models. Two important factors are the nature and lifetime of the excited state of the sensitizer. All the trinuclear ruthenium complexes investigated in this work have very short emission lifetimes, a feature which is quite different from the $[Ru(bpy)_3Mn_2]$ complexes we have studied previously.[13,17] Because of the short lifetime, it seems difficult to initiate photooxidation of the excited $[Ru(bpy)_3]^{2+}$ by an external electron acceptor. However, the desired photoinduced multistep electron transfer was achieved by attaching the $Ru(bpy)_3$ unit to nanocrystalline TiO_2 as acceptor, which resulted in long-lived charge separation, albeit with a low yield. On the other hand, since the dominant quenching responsible for the short emission lifetime of trinuclear ruthenium complexes is exchange EnT and/or oxidative quenching, it should be possible to reduce this effect by introducing an electron-donating group instead of the electron-withdrawing group on the bridging bipyridine ligand. This may increase the excited-state lifetime and allow the use of external acceptors other than TiO_2. In conclusion, polyruthenium complexes could be used as alternative electron donors in an artificial system for water oxidation or solar cells, and this study is a first attempt to construct such a system.

Experimental Section

Materials: All chemicals were purchased from Aldrich or Lancaster and used as received. All solvents were dried by standard methods. Silica gel 60 (0.043–0.063 mm, Merck, Darmstadt, Germany) was used for column chromatography. Complexes *cis*-$[RuCl_2(dmso)_4]$,[56] **1**,[31] **3**[21] and **3a**[32] were prepared as described earlier.

Mass spectrometry: Electrospray ionization mass spectrometry (ESI-MS) was performed on a Bruker Daltonics BioAPEX-94e superconducting 9.4T FTICR mass spectrometer (Bruker Daltonics, Billerica, MA, USA) in broad mode. A homebuilt apparatus controlled the direct infusion of the sample. The sample (dissolved in CH_3CN/H_2O/HOAc 49.5:49.5:1) was delivered by using a helium gas container at a pressure of 1.3 bar that pushed the sample through a 30 cm fused silica capillary of inner diameter 20 μm. The sample end of the capillary was lowered into the sample tube inside the pressurized container, and the electrospray end was coated by a conducting graphite/polymer layer[57] and connected to ground. No sheath flow or nebulizing gas was used, and the flow rate was approximately 100 nL min^{-1}. The ion source was coupled to an Analytica atomsphere/vacuum interface (Analytica of Branford, CT, USA), and a potential difference of 2–4 kV was applied across a distance of approximately 5 mm between the spraying needle and inlet capillary.

TiO_2 film preparation: To obtain a nanocrystalline TiO_2 film of uniform thickness, we used a glass rod to spread a drop of viscous TiO_2 suspension onto a microscope glass slip. After drying in air at room temperature for about 2 h, it was sintered at 420–440 °C for 30 min to form a transparent TiO_2 film. Dye sensitization of the TiO_2 film was carried out by soaking the still-hot film in an acetonitrile solution of the dye and incubating in the dark at room temperature for about 24 h. After the sensitization procedure the film was rinsed with acetonitrile to wash off the unattached dye, dried at room temperature, covered with acetonitrile and another microscope glass slip and finally sealed.

UV/Vis absorption spectroscopy: UV/Vis absorption spectra were measured on a Hewlett Packard 8453 instrument. The time-resolved measurements were performed on two similar systems. Femtosecond pulses were obtained from a Ti:Sapphire oscillator pumped by the 5 W output of a CW frequency-doubled, diode-pumped Nd:YVO_4 laser or an Ar ion laser. The oscillator, operating at a repetition rate of 82 or 76 MHz, was amplified by a regenerative Ti:Sapphire amplifier pumped by a Nd:YLF laser (1 kHz) producing about 130 fs pulses with an average energy of about 0.9 mJ per pulse and a central wavelength at 800 nm. The amplified pulses were divided into two paths: one to pump an optical parametric amplifier for generation of excitation pulses, and the other to produce white-light continuum probe pulses in a sapphire or CaF_2 plate. The mutual polarization of the pump and probe beams was set to the magic angle (54.7°) by using a polarization rotator placed in the pump beam. For signal detection, the probe beam and an identical reference beam that had no overlap with the pump beam were focused onto the entrance slit of a spectrograph, which then dispersed both beams onto a homebuilt dual photodiode array detection system. Measurements on the nanosecond to second timescale were carried out using a nanosecond laser flash photolysis setup. Excitation pulses at 480 nm (0.4 mJ, 7 ns fwhm) were obtained from a Quanta-Ray master optical parametric oscillator (MOPO) pumped by a Quanta-Ray 230 Nd:YAG laser (355 nm). The probe light was provided by a 75 W Xe arc lamp and was collinear with the excitation beam. After passing through the sample, the probe light was spectrally filtered by two monochromators and finally detected by a Hamamatsu R928 photomultiplier tube.

The time-resolved emission experiments were performed with a conventional time-correlated single-photon counting setup. Excitation was performed with laser pulses at 400 nm and 200 kHz repetition frequency at a power of <1 mW. Emission wavelengths were selected with suitable filters and detected with a Peltier-cooled detector.

Electrochemistry: Cyclic voltammetry and differential pulse voltammetry were performed with an Autolab potentiostat with an GPES electrochemical interface (Eco Chemie), a glassy carbon disk (diameter 3 mm, freshly polished) as working electrode, a platinum spiral in a compartment separated from the bulk solution by a fritted disk as counterelectrode and a nonaqueous Ag/Ag^+ electrode (CH Instruments, 0.01 M $AgNO_3$ in acetonitrile) with a potential of −0.08 V versus the ferrocenium/ferrocene (Fc^+/Fc) couple in acetonitrile as external standard. All potentials reported here are versus SCE by adding +0.380 V to the potentials measured versus the (Fc^+/Fc) couple.

Half-wave potentials ($E_{1/2}$) were determined by cyclic voltammetry as the average of the anodic and cathodic peak potentials ($E_{1/2}=(E_{pa}+E_{pc})/2$). The reversibility was determined by the peak-to-peak separations ΔE_p ($\Delta E_p = E_{pa}-E_{pc}$) and the ratio of the anodic to cathodic peak currents (i_{pa}/i_{pc}).

Solutions were prepared from dry acetonitrile (Merck, spectroscopic grade, dried with 3 Å MS) and contained ca. 1 mM of the analyte and 0.1 M tetrabutylammonium hexafluorophosphate (Fluka, electrochemical grade, dried at 373 K) as supporting electrode. The glassware used was oven-dried, assembled and flushed with argon while hot. Before all measurements the stirred solutions were bubbled with solvent-saturated argon, and the samples were kept under argon atmosphere during measurements.

EPR spectroscopy: EPR spectra were collected from a sample of complex **2** after dissolution in dry acetonitrile and freezing in liquid nitrogen. The concentration of **2** in the frozen solution was ca. 1 mM. EPR measurements were carried out on a Bruker E500 X-band spectrometer equipped with a Bruker dual-mode cavity and an Oxford Instruments temperature controller and ESR900 flow cryostat. Spectrometer configuration: See legend to Figure 2.

$[Ru(bpy)_3]^{2+}$-BPMP[$Ru_2^{II,III}$(μ-OAc)$_2$]$(PF_6^-)_4$ (2): $[RuCl_2(dmso)_4]$ (38 mg, 0.078 mmol) and NaOAc (68 mg, 0.8 mmol) were added to a solution of **3**[21] (56 mg, 0.036 mmol) in MeOH (5 mL). The mixture was refluxed for 18 h under N_2 in the dark. A saturated solution of NH_4PF_6 in methanol was added to the resulting red-brown solution. Most of the solvent was removed under reduced pressure. The residue was dissolved in CH_2Cl_2 (20 mL) and washed with water (3 × 15 mL). The organic phase was dried over Na_2SO_4. Removing the solvent afforded 51 mg (66 %) of the desired product as the PF_6^- salt. ESI-MS: *m/z*: 1996.1 $[M-PF_6^-]^+$ (calcd 1996.1), 925.6 $[M-2PF_6^-]^{2+}$ (calcd 925.6), 568.7 $[M-3PF_6^-]^{3+}$ (calcd 568.7); elemental analysis calcd (%) for $C_{73}H_{70}F_{24}N_{13}O_8P_4Ru_3\cdot 7CH_3OH$: C 40.63, H 4.18, N 7.70; found: C 40.89, H 4.21, N 7.62.

Trinuclear ruthenium(II,II,III) complex 2a: This complex was prepared in a similar way to **2**. Ligand **3a**[32] (57 mg, 0.031 mmol), $[RuCl_2(dmso)_4]$ (33 mg, 0.068 mmol) and NaOAc (31 mg, 0.38 mmol) in MeOH (10 mL) were refluxed for 18 h under N_2 in the dark. A saturated aqueous solution of NH_4PF_6 was added to the resulting red-brown solution. After three days, the brown-red solid was collected by filtration, washed with water and diethyl ether and dried under vacuum. Yield: 36 mg (47 %). ESI-MS: *m/z*: 2229.3 $[M-PF_6^-]^+$ (calcd 2229.2), 1042.1 $[M-2PF_6^-]^{2+}$ (calcd 1042.1), 646.4 $[M-3PF_6^-]^{3+}$ (calcd 646.4), 448.6 $[M-4PF_6^-]^{4+}$ (calcd 448.6); elemental analysis calcd (%) for $C_{85}H_{86}F_{24}N_{13}O_{16}P_4Ru_3\cdot NH_4PF_6\cdot 2\,MeOH\cdot 0.5\,NaPF_6$: C 38.14, H 3.61, N 7.16; found: C 38.31, H 3.53, N 7.12.

Trinuclear ruthenium(II,II,III) complex 2b: This complex was prepared by hydrolysis of complex **2a**. Compound **2a** (22 mg, 9.2 μmol) was dissolved in acetone (5 mL), and 2 M NaOH (40 μL, 80 μmol) was added. The mixture was refluxed for 2 h. After the mixture had been cooled to room temperature, 2 N HCl (0.1 mL) was added, followed by addition of excess NH_4PF_6. Acetone was removed and the residue was washed with H_2O and dried. The reaction gave **2b** in 14 mg yield. No further purification was attempted for this complex.

Acknowledgement

Financial support for this work was provided by the Swedish Energy Agency, the Knut and Alice Wallenberg Foundation, the Swedish Research Council for Engineering Sciences (TFR), the Swedish Science Research Council for Natural Science (NFR), the Swedish Research Council (VR) and DESS.

[1] T. J. Meyer, *Acc. Chem. Res.* **1989**, *22*, 163–170.
[2] V. L. Pecoraro, M. J. Baldwin, A. Gelasco, *Chem. Rev.* **1994**, *94*, 807–826.
[3] R. Manchanda, G. W. Brudvig, R. H. Crabtree, *Coord. Chem. Rev.* **1995**, *144*, 1–38.
[4] A. J. Bard, M. A. Fox, *Acc. Chem. Res.* **1995**, *28*, 141–145.
[5] a) J. Limburg, V. A. Szalai, G. W. Brudvig, *J. Chem. Soc. Dalton Trans.* **1999**, 1353–1361; b) J. Limburg, J. S. Vrettos, H. Chen, J. C. de Paula, R. H. Crabtree, G. W. Brudvig, *J. Am. Chem. Soc.* **2001**, *123*, 423–430.
[6] W. Ruettinger, G. C. Dismukes, *Chem. Rev.* **1997**, *97*, 1–24.
[7] M. Yagi, M. Kaneko, *Chem. Rev.* **2001**, *101*, 21–35.
[8] a) L. Sun, L. Hammarström, B. Åkermark, S. Styring, *Chem. Soc. Rev.* **2001**, *30*, 36–49; b) L. Hammarström, *Curr. Opin. Chem. Biol.* **2003**, *7*, 666.
[9] V. K. Yachandra, K. Sauer, M. P. Klein, *Chem. Rev.* **1996**, *96*, 2927–2950.
[10] G. C. Dismukes, *Chem. Rev.* **1996**, *96*, 2909–2926.
[11] S. Mukhopadhyay, S. K. Mandal, S. Bhaduri, W. Armstrong, *Chem. Rev.* **2004**, *104*, 3981–4026.
[12] M. Yagi, K. Narita, *J. Am. Chem. Soc.* **2004**, *126*, 8084–8085.
[13] L. Sun, M. K. Raymond, A. Magnuson, D. LeGourrierec, M. Tamm, M. Abrahamsson, P. H. Kenez, J. Mårtensson, G. Stenhagen, L. Hammarström, S. Styring, B. Åkermark, *J. Inorg. Biochem.* **2000**, *78*, 15–22.
[14] A. Johansson, M. Abrahamsson, A. Magnuson, P. Huang, J. Mårtensson, S. Styring, L. Hammarström, L. Sun, B. Åkermark, *Inorg. Chem.* **2003**, *42*, 7502–7511.
[15] D. Burdinski, E. Bothe, K. Wieghardt, *Inorg. Chem.* **2000**, *39*, 105–116.
[16] D. Burdinski, K. Wieghardt, S. Steenken, *J. Am. Chem. Soc.* **1999**, *121*, 10781–19787.
[17] L. Sun, H. Berglund, R. Davydov, T. Norrby, L. Hammarström, P. Korall, A. Börje, C. Philouze, K. Berg, A. Tran, M. Andersson, G. Stenhagen, J. Martensson, M. Almgren, S. Styring, B. Åkermark, *J. Am. Chem. Soc.* **1997**, *119*, 6996–7004.
[18] L. Sun, L. Hammarström, T. Norrby, H. Berglund, R. Davydov, M. Andersson, A. Börje, P. Korall, C. Philouze, M. Almgren, S. Styring, B. Åkermark, *Chem. Commun.* **1997**, *119*, 607–608.
[19] A. Magnuson, H. Berglund, P. Korall, L. Hammarström, B. Åkermark, S. Styring, L. Sun, *J. Am. Chem. Soc.* **1997**, *119*, 10720–10725.
[20] H. Berglund-Baudin, L. Sun, R. Davidov, M. Sundahl, S. Styring, B. Åkermark, M. Almgren, L. Hammarström, *J. Phys. Chem. A* **1998**, *102*, 2512–2518.
[21] L. Sun, M. Burkitt, M. Tamm, M. K. Raymond, M. Abrahamsson, D. LeGourrierec, Y. Frapart, A. Magnuson, P. H. Kenez, P. Brandt, A. Tran, L. Hammarström, S. Styring, B. Åkermark, *J. Am. Chem. Soc.* **1999**, *121*, 6834–6842.
[22] A. Magnuson, Y. Frapart, M. Abrahamsson, O. Horner, B. Åkermark, L. Sun, J. J. Girerd, L. Hammarström, S. Styring, *J. Am. Chem. Soc.* **1999**, *121*, 89–96.
[23] L. Hammarström, L. Sun, B. Åkermark, S. Styring, *Biochim. Biophys. Acta* **1998**, *1365*, 193–199.
[24] M. L. A. Abrahamsson, H. Berglund-Baudin, A. Tran, C. Philouze, K. E. Berg, M. K. Raymond-Johansson, L. Sun, B. Åkermark, S. Styring, L. Hammarstöm, *Inorg. Chem.* **2002**, *41*, 1534–1544.
[25] K. E. Berg, A. Tran, M. K. Raymond, M. Abrahamsson, J. Wolny, S. Redon, M. Andersson, L. Sun, S. Styring, L. Hammarström, H. Toftlund, B. Åkermark, *Eur. J. Inorg. Chem.* **2001**, *4*, 1019–1029.
[26] P. Huang, A. Magnuson, R. Lomoth, M. Abrahamsson, M. Tamm, L. Sun, B. van Rotterdam, J. Park, L. Hammarström, B. Åkermark, S. Styring, *J. Inorg. Biochem.* **2002**, *91*, 159–172.
[27] S. W. Gersten, G. J. Samuels, T. J. Meyer, *J. Am. Chem. Soc.* **1982**, *104*, 4029–4030.
[28] R. A. Binstead, C. W. Chronister, J. Ni, C. M. Hartshorn, T. J. Meyer, *J. Am. Chem. Soc.* **2000**, *122*, 8464–8473.
[29] E. L. Lebeau, S. A. Adeyemi, T. J. Meyer, *Inorg. Chem.* **1998**, *37*, 6474–6484.
[30] C. Sens, I. Romero, M. Rodriguez, A. Llobet, T. Parella, J. Benet-Buchhola, *J. Am. Chem. Soc.* **2004**, *126*, 7798–7799.
[31] R. Lomoth, A. Magnuson, Y. Xu, L. Sun, *J. Phys. Chem. A* **2003**, *107*, 4373–4380.
[32] J. Pan, Y. Xu, G. Benkö, Y. Feyziyev, S. Styring, L. Sun, B. Åkermark, T. Polivka, V. Sundström, *J. Phys. Chem. B* **2004**, *108*, 12904–12910.
[33] M. Sjödin, S. Styring, H. Wolpher, Y. Xu, L. Sun, L. Hammarström, *J. Am. Chem. Soc.* **2005**, *127*, 3855–3863.
[34] B. M. Peek, G. T. Ross, S. W. Edward, G. T. Meyer, T. J. Meyer, B. W. Erickson, *Int. J. Peptide Protein Res.* **1991**, *38*, 114–123.
[35] J. L. Bear, B. Han, S. Huang, *J. Am. Chem. Soc.* **1993**, *115*, 1175–1177.
[36] K. Kalyanasundaram, *Photochemistry of Polypyridine and Porphyrin Complexes*, Academic Press, London, **1992**, pp. 106–116.
[37] A. Juris, V. Balzani, F. Barigelletti, S. Campagna, P. Belser, A. Von Zelewsky, *Coord. Chem. Rev.* **1988**, *84*, 85–277.
[38] G. Eilers, Y. Xu, unpublished results.
[39] Ultrafast intersystem crossing to a triplet, albeit strongly mixed with singlets, would occur also in Ru_2 complex **1**, so that the same excited state would be obtained both by direct excitation and by possible energy transfer from the $[Ru(bpy)_3]^{2+}$ triplet.
[40] T. Förster, *Discuss. Faraday Soc.* **1959**, *27*, 7.
[41] H. Sun, A. Yoshimura, M. Z. Hoffman, *J. Phys. Chem.* **1994**, *98*, 5058–5064.
[42] R. A. Malone, D. F. Kelley, *J. Chem. Phys.* **1991**, *95*, 8970–8976.
[43] J. Andersson, F. Puntoniero, S. Serroni, A. Yartsev, T. Pascher, T. Polivka, S. Campagna, V. Sundström, *Faraday Discuss.* **2004**, *127*, 295–305.
[44] S. Wallin, J. Davidsson, J. Modin, L. Hammarström, *J. Phys. Chem. A*, **2005**, *109*, 4697–4704.
[45] L. F. Cooley, S. L. Larson, C. M. Elliot, D. F. Kelley, *J. Phys. Chem.* **1991**, *95*, 10694–10700.
[46] L. A. Kelly, M. A. J. Rodgers, *J. Phys. Chem.* **1995**, *99*, 13132–13140.
[47] A. Hagfeldt, M. Grätzel, *Acc. Chem. Res.* **2000**, *33*, 269–277.
[48] G. Benkö, J. Kallioinen, J. E. Korppi-Tommola, A. P. Yartsev, V. Sundström, *J. Am. Chem. Soc.* **2002**, *124*, 489–493.
[49] J. Kallioinen, G. Benkö, V. Sundström, J. Korppi-Tommola, A. Yartsev, *J. Phys. Chem. B* **2002**, *106*, 4396–4404.
[50] J. B. Asbury, E. Hao, Y. Wang, H. N. Ghosh, T. Lian, *J. Phys. Chem. B* **2001**, *105*, 4545–4557.
[51] R. Ghanem, Y. Xu, J. Pan, T. Hoffmann, J. Andersson, T. Polivka, T. Pascher, S. Styring, L. Sun, V. Sundström, *Inorg. Chem.* **2002**, *41*, 6258–6266.
[52] R. Argazzi, C. A. Bignozzi, T. A. Heimer, F. N. Castellano, G. J. Meyer, *J. Am. Chem. Soc.* **1995**, *117*, 11815–11816.
[53] P. Bonhôte, J.-E. Moser, R. Humphry-Baker, N. Vlachopoulos, S. M. Zakeeruddin, L. Walder, M. Grätzel, *J. Am. Chem. Soc.* **1999**, *121*, 1324–1336.
[54] C. J. Kleverlaan, M. T. Indelli, C. A. Bignozzi, L. Pavanin, F. Scandola, G. M. Hasselman, G. J. Meyer, *J. Am. Chem. Soc.* **2000**, *122*, 2840–2849.
[55] S. A. Haque, Y. Tachibana, D. R. Klug, J. R. Durrant, *J. Phys. Chem. B* **1998**, *102*, 1745–1749.
[56] I. P. Evans, A. Spencer, G. Wilkinson, *J. Chem. Soc. Dalton Trans.* **1973**, 204–209.
[57] S. Nilsson, M. Wetterhall, J. Bergquist, L. Nyholm, K. E. Markides, *Rapid Commun. Mass Spectrom.* **2001**, *15*, 1997–2000.

Received: May 27, 2005
Published online: September 15, 2005

